

TRMM RE-ENTRY PLANNING: ATTITUDE DETERMINATION AND CONTROL DURING THRUSTER MODES

Keith DeWeese
NASA Goddard Space Flight Center
Greenbelt, MD 20771
keith.d.deweese@nasa.gov

ABSTRACT

The Tropical Rainfall Measuring Mission (TRMM) spacecraft has been undergoing design for a controlled re-entry to Earth. During simulation of the re-entry plan, there was evidence of errors in the attitude determination algorithms during thruster modes. These errors affected the burn efficiency, and thus planning, during re-entry. During thruster modes, the spacecraft attitude is controlled off of integrated Gyro Error Angles that were designed to closely follow the nominal spacecraft pointing frame (Tip Frame). These angles, however, were not exactly mapped to the Tip Frame from the Body Frame. Additionally, in the initial formulation of the thruster mode attitude determination algorithms, several assumptions and approximations were made to conserve processor speed. These errors became noticeable and significant when simulating burns of much longer duration (~10 times) than had been produced in flight. A solution is proposed that uses attitude determination information from a propagated extended Kalman filter that already exists in the TRMM thruster modes. This attitude information is then used to rotate the Gyro Error Angles into the Tip Frame. An error analysis is presented that compares the two formulations. The new algorithm is tested using the TRMM High-Fidelity Simulator and verified with the TRMM Software Testing and Training Facility. Simulation results for both configurations are also presented.

INTRODUCTION

The Tropical Rainfall Measurement Mission (TRMM) is a joint NASA/NASDA mission that was launched on November 27, 1997 from Tanegashima Space Center, Japan. The spacecraft is three-axis stabilized, currently in a near circular 402 km orbit at 35 degree inclination. The spacecraft sensor complement is described in Andrews, et al¹.

Spacecraft Control Modes

The spacecraft Attitude Control System (ACS) consists of many control modes for various aspects of its mission¹. Full description of the modes is beyond the scope of this paper, but specific modes will be summarized here for completeness. The modes are divided into thruster and non-thruster modes depending on whether the thrusters are the primary actuator of the mode. The thruster modes have a control frequency of 8 Hz while non-thruster modes run at a 2 Hz control frequency. For regular mission activities (such as an orbit raising burn), the spacecraft enters a thruster mode via a ground command. The specified burn takes place and the spacecraft exits thruster mode automatically. After exiting, the spacecraft proceeds to two intermediate reaction wheel modes before entering the nominal mission mode. The spacecraft enters the first intermediate mode, Yaw Acquisition, and then moves to Earth Acquisition mode. After reaching a certain position, rate, and time threshold, the spacecraft returns to the PID (Proportional+Integral+Derivative) controlled mission mode.

Mission mode is designed to control the spacecraft to a near nadir frame called the Tip Frame². The Tip Frame is found from the bisection of the angle marked by the horizon lines. In the initial design, TRMM used an Earth Sensor Assembly¹ for Tip Frame attitude determination. This design was changed to a Kalman Filter attitude determination algorithm as a contingency during Mission Mode once the orbit was raised from the initial 350 km to the current 402 km³.

Attitude Knowledge During Control Modes

Although the nominal Mission Mode is controlled based on the Kalman Filter as the attitude knowledge, the thruster modes are not. The two thruster modes are controlled off of gyro rate information alone. The rate errors from the gyros are integrated into position errors for use in the thruster mode PD (Proportional+Derivative) controllers. These Gyro Error Angles (GEAs) were known to drift during extended Mission Mode operations. To reduce the error of the GEAs when entering thruster modes, the standard TRMM procedure called for zeroing the GEAs just prior to entering the thruster modes. Since the spacecraft had nominally been in Mission Mode before entering the thruster mode, the Tip Frame error could be assumed to be insignificant with respect to the thruster mode controller dead band³. The Delta-V Mode burns themselves were also typically of very short duration (less than 3 minutes), so the integrated errors from integrating the gyro rates were also small.

Nominal Re-entry Plan

The details of the nominal re-entry plan are beyond the scope of this paper. In summary, when the point of controlled re-entry is reached, the TRMM spacecraft would begin a drag-down descent from the normal operating 402 km circular orbit to an altitude of 330 km. At this point, a sequence of burns at apogee would be initiated to bring the spacecraft into the Earth's atmosphere. Burn 1 would take the spacecraft from the 330 km circular orbit to an eccentric 320 x 220 km orbit. The spacecraft would stay in this orbit between one and seven days. Burn 2 would then bring the perigee down to 130 km. One orbit later, burn 3 would be executed to bring the spacecraft into the Earth's atmosphere. Between Burn 2 and Burn 3, the atmospheric torques on the spacecraft would overwhelm the reaction wheel actuators, and the spacecraft would lose attitude control. To combat this, the spacecraft would enter a Delta-H thruster mode for attitude control at low perigees (below 180 km).

ANALYSIS TOOLS

During mission design, two simulation programs were introduced for systems validation. The High-Fidelity simulator (HiFi) was developed to test the attitude control algorithms. This simulator includes mathematical models of the spacecraft sensing and actuating hardware as well as standard orbital mechanics models (two body orbital mechanics, magnetic field, gravity, atmospheric density).

The Software Testing and Training Facility (STTF) was created to test the flight software on replicas of the actual spacecraft flight hardware. The inclusion of the actual flight hardware and software gives the controls analyst a better representation of the controller environment.

Extensive work was done by the TRMM GN&C Re-entry team to calibrate the two simulation platforms to align them with flight data. Adjustments were made to the spacecraft and environment model parameters to more closely match flight data. Details of this work and the results of the simulations is the subject of a future paper. Once these modifications were in place, simulations were run in the HiFi and the STTF of the nominal re-entry plan.

ATTITUDE ERRORS IN NOMINAL RE-ENTRY SIMULATIONS

The re-entry simulations were processed in two phases. Since, in the nominal plan, there could be as much as seven days' time between Burn 1 and Burn 2, this seemed like a logical place to separate the re-entry phases. Initial analyses of the Burn 1 simulations did not show anomalous results. The spacecraft enters the burn normally, burns for the full expected duration, and exits nominally into the post-thruster mode phases.

During analysis of the Burn2-Delta-H-Burn3 re-entry sequence, an unacceptably large pointing error was found during the third burn. This error was as much as 30 degrees off of the nominal Tip Frame in the pitch (Y) and yaw (Z) axes, causing unacceptable alignment of the thrust vector with the anti-velocity vector (misalignment > 15 degrees). Burn 2 appears nominal, as did Burn 1. Errors begin to be noticeable during Delta-H Mode, but these were initially attributed to the design of the controller; Delta-H mode was not designed to track orbit rate, only to shed momentum using the thrusters. Burn 3 is where the very large Tip Frame errors became an issue. The error was first apparent during STTF runs where an older version of the aerodynamic torque model was being used. Use of the updated aerodynamic torque models decreased, but did not eliminate, the errors (Figure 1). In the figure, the Tip Frame errors show that the spacecraft thrust vector would no longer be aligned with the anti-velocity vector, causing unacceptable burn inefficiencies. The HiFi simulation showed similar results (Figure 2).

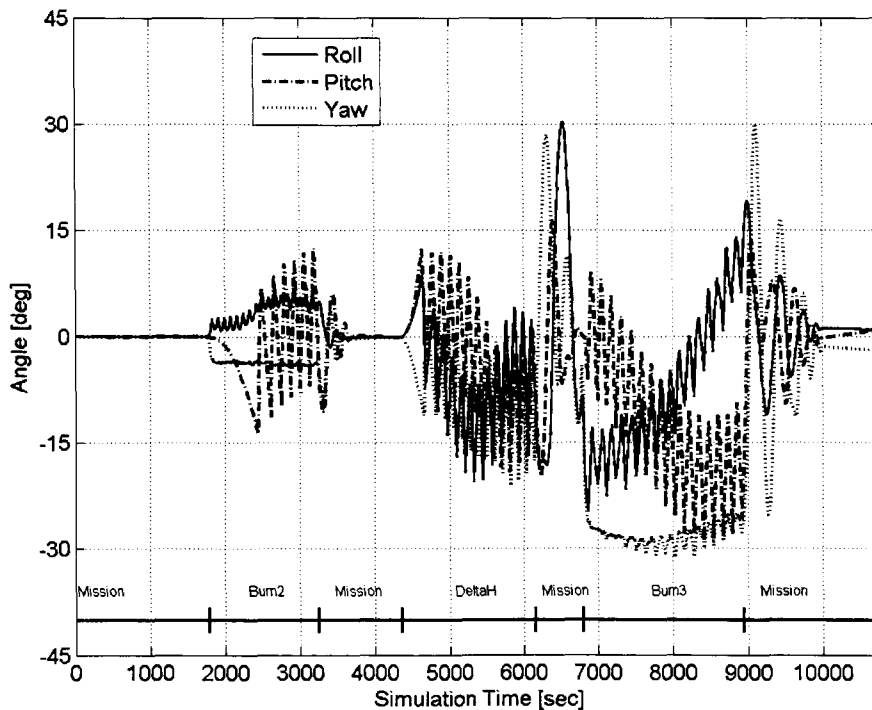


Figure 1. TRMM Tip Frame Error Angles: STTF Initial Analysis

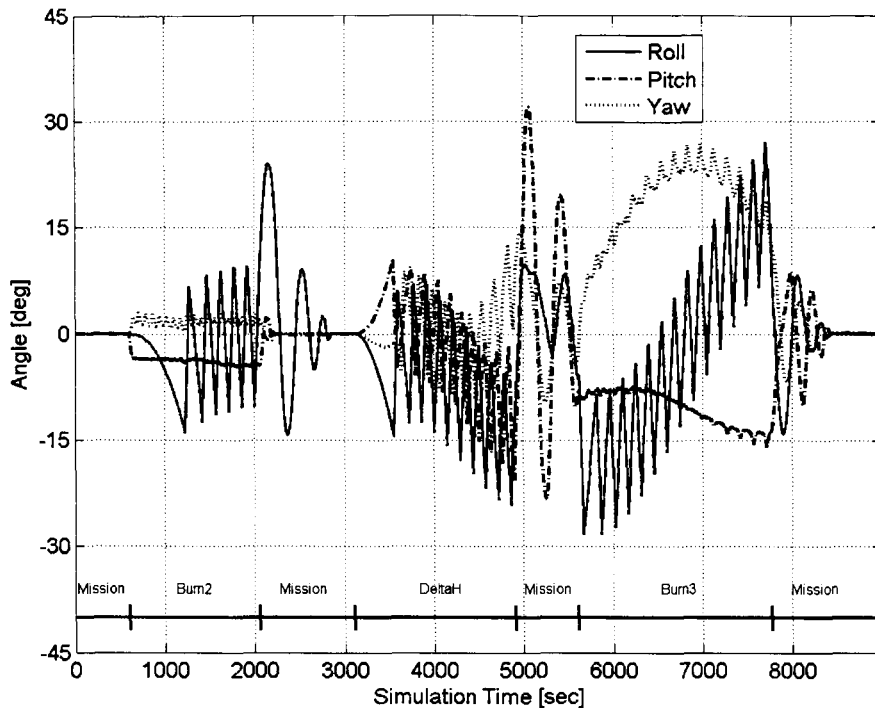


Figure 2. TRMM Tip Frame Error Angles: HiFi Initial Analysis

DIAGNOSING THE PROBLEM: ATTITUDE DETERMINATION VS. ATTITUDE CONTROL

The two most likely sources of this type of large drift in the Tip Frame are incorrect controller design and incorrect attitude determination. To investigate attitude control, the controller error signals are scrutinized. During all phases of the simulation, the controller is able to keep the position errors below the pointing requirement (< 15 degrees). In particular, the spacecraft is controlled successfully during all thruster modes (Figures 3-4). The Tip Frame errors that show up at the end of Delta-H Mode and Burn 2 are compensated by the nominal mission mode controller upon entering Mission Mode. The Kalman filter maintains pointing knowledge during thruster modes (the spacecraft returns to nominal Tip Frame pointing after each thruster mode), but the attitude knowledge during thruster modes seems to be in error. Thus, it is unlikely that attitude control is the source of the Tip Frame drift, and attitude determination should be analyzed.

As previously mentioned, during thruster modes the ACS is controlling off of the integrated Gyro Error Angles (GEAs). Over the duration of the Burn2-Delta-H-Burn3 sequence, the GEAs drifted from the nominal Tip Frame with which the Delta-V burns need to be aligned (Figures 5-6). Notice that during the thruster modes, the spacecraft controls to the GEAs. Upon exiting the thruster mode, the GEAs almost instantaneously go to a large nonzero value (~ 25 degrees). This is due to the different attitude determination algorithm that is occurring during Mission Mode, the Kalman Filter. Thus the problem is one of attitude determination during thruster modes, not attitude control. In order to better understand the differences between the Gyro Error Angle calculations and the actual Tip Frame of the spacecraft, the details of the original algorithm derivation were revisited.

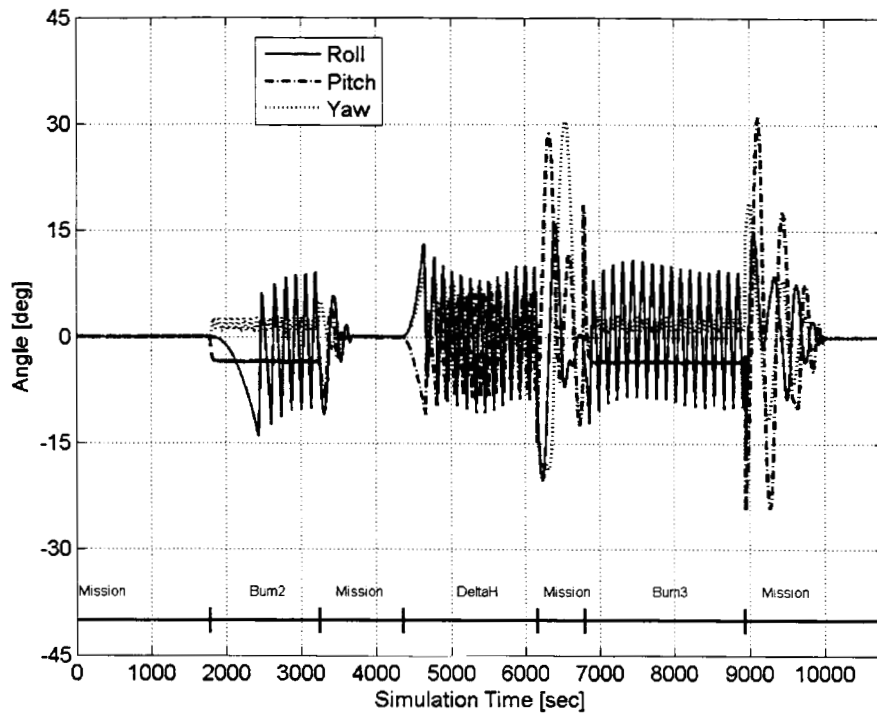


Figure 3. TRMM Controller Position Error Angles: STTF Initial Analysis

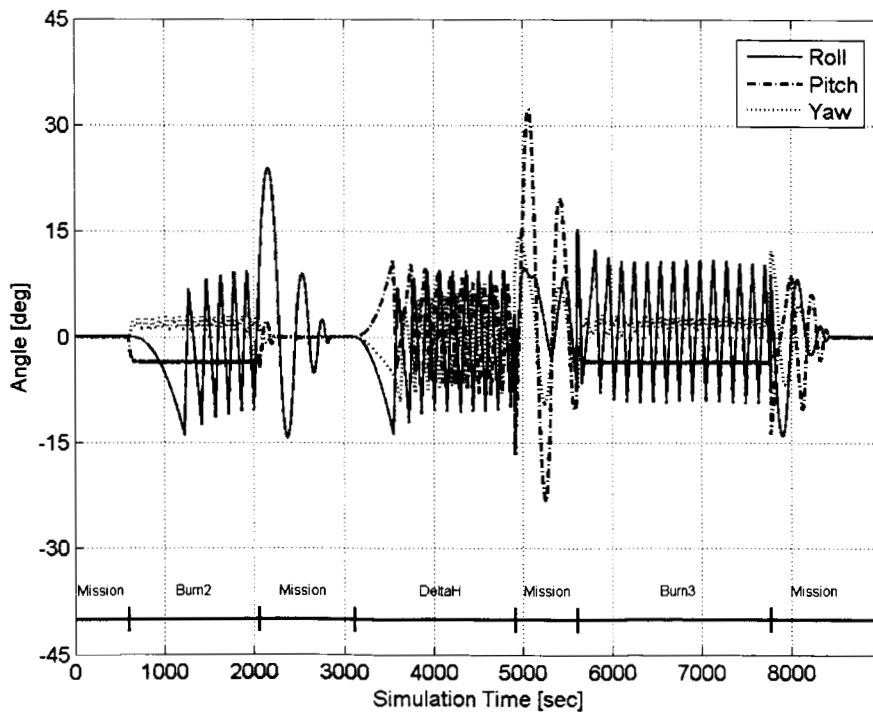


Figure 4. TRMM Controller Position Error Angles: HiFi Initial Analysis

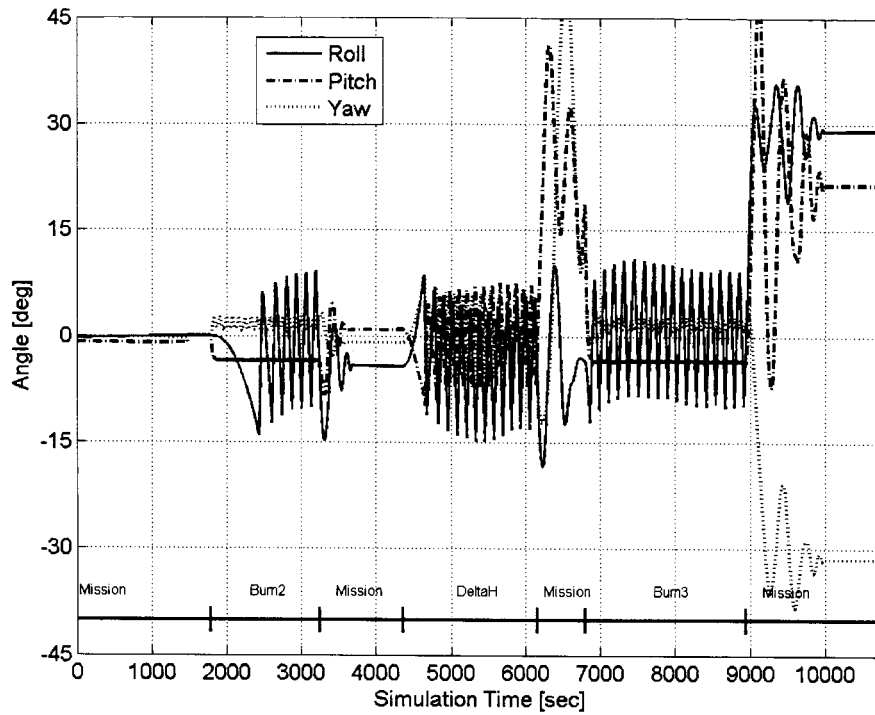


Figure 5. TRMM Gyro Error Angles: STTF Initial Analysis

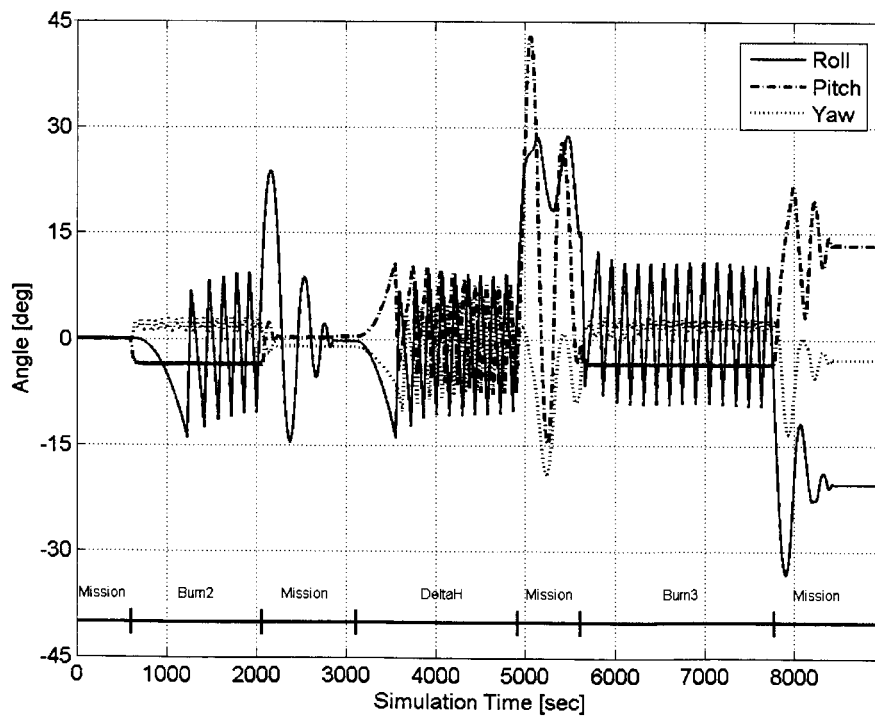


Figure 6. TRMM Gyro Error Angles: HiFi Initial Analysis

TRMM THRUSTER MODE ATTITUDE DETERMINATION METHODS

As previously mentioned, TRMM uses two methods of attitude determination; one for control in thruster modes and one for nominal modes. Details of the TRMM ACS control methodology can be found in the algorithm document⁴.

Nominal Modes

During Mission Mode operation, the TRMM spacecraft uses a Kalman filter to determine spacecraft attitude¹. Briefly, the process is:

- Use a Kalman filter and information from gyros, magnetometers, and sun sensors to determine attitude information.
- Use this information to determine the Tip-to-Body Frame transformation matrix.
- Use this Tip-to-Body matrix to compute the desired body rate (ω_{Body}) in the body frame and in the inertial frame (ω_0).

Thruster Modes

During thruster modes (Delta-V and Delta-H) the ACS uses a small angle approximation to compute ω_{Body} in the body frame. Originally, the reason for the differences was concern about computation time during the 8Hz modes. This concern is no longer warranted, thus the thruster modes can now use a more accurate propagated Kalman quaternion for attitude determination¹. The changes in thruster mode:

- Use the propagated Kalman filter attitude information to determine the Tip-to-Body transformation matrix
- Use this Tip-to-Body matrix to compute ω_{Body} in the body frame and in the inertial frame (ω_0).

Delta-H Mode

In addition to the differences discussed above, the design of the Delta-H Mode controller differs from the Delta-V Mode controller in one very significant way. The original Delta-H controller was never designed to track orbit rate. It was to be used only for very short, momentum dumping burns. However, longer duration Delta-H burns would allow the spacecraft to drift from the Tip Frame at roughly 4 degrees per minute. Over a nominal 30 minute Delta-H, that would require the spacecraft to correct for a 120 degree offset from the Tip Frame upon entering mission mode. To minimize power consumption between thruster modes, the decision was made to modify the Delta-H Mode controller to also track the orbit rate.

ERRORS IN ATTITUDE DETERMINATION

To start the GEA calculation analysis, we assume that the GEAs are nearly equal to the position error in mission mode just before Burn 2 (i.e. the errors are negligible in this analysis). This assumption can be made if the position error is nearly equal to zero ($P_{\text{ERR}} \sim 0$) just before Burn 2 when the GEAs are reset to zero to eliminate any integration bias. Due to the limited time between thruster modes in the final burn sequence, the amount of time in Earth Acquisition Mode was decreased to one control cycle. Thus, upon

entering Mission Mode, the position errors could be large (on the order of 10 degrees). Because of this, the Gyro Error Angles are not going to be reset to zero after Burn 2.

In addition to this assumption, a couple of observations should be made:

1. Both the propagation of the Tip Frame errors and the gyro rate error calculations use the same gyro measured rate: $\omega_g(t)$
2. The desired spacecraft body rate (ω_0) is calculated the same way in all modes.

Flatley² describes the derivation of the true Tip Frame rate errors, which can be determined from orbit information. In this derivation, Flatley uses small angle approximations to alleviate the computation burden on the flight processor. In order to determine the nature and magnitude of the errors that these assumptions introduce over an extended period of time, the derivation will be performed again with no approximations for comparison. The following derivation comes nearly entirely from Flatley.

The rotation of the desired body rates from the Tip Frame to the body frame can be determined through a [3-2-1] Euler rotation by the following process:

1. Multiply the desired body rate vector (ω_0) by the yaw transformation matrix (R_z) and add the Tip Frame yaw rate ($\dot{\psi}$).
2. Multiply that result by the pitch transformation matrix (R_y) and add the Tip Frame pitch rate ($\dot{\theta}$).
3. Multiply that result by the roll transformation matrix (R_x) and add the Tip Frame roll rate ($\dot{\phi}$).

This process leads to an equation of the measured gyro rates in terms of the rotation matrices and the Tip Frame rates:

$$\omega_g = R_x \{ R_y (R_z \omega_0 + [0 \ 0 \ \dot{\psi}]^T) + [0 \ \dot{\theta} \ 0]^T \} + [\dot{\phi} \ 0 \ 0]^T \quad [1]$$

$$= R_x R_y R_z \omega_0 + R_x R_y [0 \ 0 \ \dot{\psi}]^T + R_x [0 \ \dot{\theta} \ 0]^T + [\dot{\phi} \ 0 \ 0]^T \quad [2]$$

$$= R_x R_y R_z \omega_0 + \begin{bmatrix} 1 & 0 & -\sin(\theta) \\ 0 & \cos(\phi) & \sin(\phi)\cos(\theta) \\ 0 & -\sin(\phi) & \cos(\phi)\cos(\theta) \end{bmatrix} \begin{bmatrix} \dot{\phi} \\ \dot{\theta} \\ \dot{\psi} \end{bmatrix} \quad [3]$$

Define the matrix multiplying the Tip Frame rates as M . This matrix has an inverse when θ is not equal to $\pi/2$. In this case, the Tip Frame rates can be solved for:

$$\begin{bmatrix} \dot{\phi} \\ \dot{\theta} \\ \dot{\psi} \end{bmatrix} = \dot{E} = M^{-1} [\omega_g - R_x R_y R_z \omega_0] \quad [4]$$

where

$$\mathbf{M}^{-1} = \begin{bmatrix} 1 & \tan(\theta)\sin(\phi) & \tan(\theta)\cos(\phi) \\ 0 & \cos(\phi) & -\sin(\phi) \\ 0 & \sin(\phi)/\cos(\theta) & \cos(\phi)/\cos(\theta) \end{bmatrix} \quad [5]$$

The matrices R_x , R_y , and R_z are rotation matrices about each axis through the appropriate angle. The term in brackets [...] in Equation [4] is of special note. It is the difference between the measured gyro rates and the desired body rate in the body frame. The controller attempts to null this term, which is why it is referred to as the control rate in the body, or Body-Rate-Control⁴. To determine the errors in the Tip Frame associated with this rate not being nulled instantaneously, the rate must be transformed to the Tip Frame coordinates. This conversion is where the inverse of the matrix \mathbf{M} is involved.

In the original derivation, it was assumed that the roll and pitch errors would be small, thus resulting in the matrix \mathbf{M} (and its inverse) being equal to identity. As previously mentioned, this was primarily done to alleviate some of the processor burden on the flight computer. The simplifications can be seen in the original implemented Gyro Error Angle rate computations ($\dot{\mathbf{e}}_g$):

$$\dot{\mathbf{e}}_g = [\omega_g - \mathbf{R}_x\mathbf{R}_y\mathbf{R}_z\omega_0] \quad [6]$$

Thus, the difference between the actual Tip Frame rates and the Gyro Error Angle rates are given by:

$$\dot{\mathbf{E}} - \dot{\mathbf{e}}_g = (\mathbf{M}^{-1} - \mathbf{I}) [\omega_g - \mathbf{R}_x\mathbf{R}_y\mathbf{R}_z\omega_0] \quad [7]$$

The matrix subtraction that multiplies the Body-Rate-Control term in equation [7] results in the following matrix.

$$(\mathbf{M}^{-1} - \mathbf{I}) = \begin{bmatrix} 0 & \tan(\theta)\sin(\phi) & \tan(\theta)\cos(\phi) \\ 0 & \cos(\phi) - 1 & -\sin(\phi) \\ 0 & \sin(\phi)/\cos(\theta) & \cos(\phi)/\cos(\theta) - 1 \end{bmatrix} \quad [8]$$

This error matrix directly influences the differences between the Gyro Error Angle calculations and the true Tip Frame attitude at each time step. From Equation 7, the error between the true Tip Frame rates and the GEA rates increases as the gyro rate increases. Also, from Equation 7, the error also increases with increasing position deviations in the Tip Frame. Since thruster mode controllers allow relatively large excursions in position and rate, these effects are significant. These errors are manifested into the integrated GEAs in the form of position errors which, in turn, affect the rate errors through Equation 7. It is interesting that, in this 3-2-1 Euler sequence, the 1st component of the term in brackets (roll rate error) does not influence the errors in the pitch and yaw axis rates in the Tip Frame.

GYRO ERROR ANGLE CALCULATION CORRECTION

As mentioned above, in order to track the Tip Frame, the rate error of the spacecraft in the body frame needs to be rotated into the Tip Frame before it is integrated. This conversion can be completed by pre-multiplying the Body-Rate-Control term by the inverse of the matrix \mathbf{M} . Thus, instead of the currently implemented rate error computation given in Equation 6, the new GEA rate error would be computed from:

$$\dot{\mathbf{e}}_g = \mathbf{M}^{-1} [\boldsymbol{\omega}_g - \mathbf{R}_x \mathbf{R}_y \mathbf{R}_z \boldsymbol{\omega}_0] \quad [9]$$

Ideally, this change would allow the Gyro Error Angles to track the Tip Frame during all modes, thus allowing the controller during Delta-V mode to maintain target on the Tip Frame. However, this correction requires knowledge of the Tip Frame angle errors, which are not directly measured. These angles go into the inverse of the \mathbf{M} matrix. In order to implement Equation 9, we will use the Gyro Error Angles that are calculated from the previous time step. This implementation will introduce errors into the computation but, as will be seen in the simulation results, these errors are acceptable.

SIMULATION RESULTS

Upon implementing the above corrections into the HiFi and STTF simulators, the Burn2-Delta-H-Burn 3 sequence was re-simulated. In both the STTF and HiFi, the Tip Frame error angles have been significantly reduced (Figures 7-8). During Delta-H Mode and Burn 3, the Tip Frame error angles do not drift and they stay within +/-15 degrees, the deadband of the controller. Also, the error angles during Delta-H Mode do not show the 4 degrees per minute drift that would indicate a lack of orbit rate tracking. In the plots, the 4-5 degree hangoff during the burns is due to unequal thrusters and the PD controller. This type of hangoff error is typical for these applications.

Just as in the pre-corrected simulations, the controller operates normally in the corrected simulations (Figures 9-10). Evidence of the correction is apparent in the plots of the Gyro Error Angles of the corrected simulations (Figures 11-12). The drift that had been seen in the pre-corrected simulations (Figures 5-6) has been greatly reduced.

CONCLUSIONS

The TRMM spacecraft must maintain adequate pointing during the difficult second phase of the re-entry plan. The previous implementation of the thruster mode attitude determination algorithm is not sufficient for the pointing requirements during re-entry. Various approximations and simplifications in the algorithm introduce errors that prohibit the required pointing during long duration thruster mode activity. The correction to the thruster mode ACS algorithm uses the onboard propagated Kalman Filter in conjunction with a more precise attitude determination calculation for the Gyro Error Angles. This modification has allowed the spacecraft to successfully meet the re-entry pointing requirements using existing onboard hardware and software elements. The changes that are required have been tested in two separate high fidelity simulations to verify this success.

REFERENCES

1. Andrews, S.F., Morgenstern, W.M., "Design, Implementation, Testing, and Flight Results of the TRMM Kalman Filter," AIAA paper 98-4509, August 1998.
2. Flatley, T.W., "TRMM Yaw," NASA Memo, November 1992.
3. Andrews, S.F., Bilanow, S., "Recent Results of the TRMM Kalman Filter," AIAA Paper 2002-5047, August 2002.
4. Bracken, J., D'Agostino, J., Barnes, K., "TRMM ACS Algorithm Document, Build 5.3," NASA Mission Document, November 1996.